

Original Article

Image quality of coronary arteries on non-electrocardiography-gated high-pitch dual-source computed tomography in children with congenital heart disease

Yuichiro Kanie¹, Shuhei Sato¹, Akihiro Tada¹, Susumu Kanazawa¹

1. Department of Radiology, Okayama University Medical School, 2-5-1 Kitaku Shikatacho,
Okayama 700-8558, Japan

Corresponding Author:

Yuichiro Kanie

E-mail: yuichirokanie@gmail.com

Tel.: +81-86-235-7313; Fax: +81-86-235-7316

Acknowledgments

The authors would like to express our appreciation to Mr. Noriaki Akagi (Division of Radiology, Okayama University Hospital) for his technical advice.

Abstract

Purpose: This study aimed to evaluate image quality of coronary artery imaging on non-electrocardiography (ECG)-gated high-pitch dual-source computed tomography (DSCT) in children with congenital heart disease (CHD) and to assess factors affecting image quality.

Materials and Methods: We retrospectively reviewed the records of 142 children with CHD who underwent non-ECG-gated high-pitch DSCT. The subjective image quality of the proximal coronary segments was graded using a five-point scale. A score < 3 represented a non-diagnostic image. Age, body weight, and heart rate were compared between the two groups: patients with good diagnostic image quality in all four segments and patients with at least one segment with non-diagnostic image quality. Predictors of image quality were assessed by multivariate logistic regression, including age, body weight, and heart rate.

Results: Four-hundred-fifty-seven of the 568 segments (80.5%) had diagnostic image quality. Patients with non-diagnostic segments were significantly younger (21.6 ± 25.5 months), had lower body weight (7.82 ± 5.00 kg), and a faster heart rate (123 ± 23.7 beats/min) (each $p < 0.05$) than patients with diagnostic image quality in all four segments (30.6 ± 20.7 months, 10.3 ± 4.00 kg, and 113 ± 21.6 beats/min, respectively; each $p < 0.05$). The multivariate logistic regression revealed that body weight (odds ratio, 1.228; $p = 0.029$) was a significant predictor of image quality.

Conclusion: Non-ECG-gated high-pitch DSCT provided adequate image quality of the proximal coronary segments in children with CHD. Lower body weight was a factor that led to poorer image quality of the coronary arteries.

Keywords: congenital heart disease, high pitch, dual source CT, non-ECG-gated, coronary CT angiography

Introduction

The basic role of computed tomography angiography (CTA) in children with congenital heart disease (CHD) is to assess the heart anatomy, arterial system, pulmonary arterial system, coronary arteries, and syndromes including asplenia, polysplenia, and so on. The incidence of coronary artery anomalies (CAAs) is approximately 1.0% in the population [1]. CAAs are often associated with CHD. Presurgical identification of CAAs is clinically important to prevent potential coronary-artery–related complications in children with CHD, such as transposition of the great artery (TGA) or tetralogy of Fallot. Coronary artery stenosis or occlusion may occur in 6.7% of patients who underwent a switch operation for TGA [2]. Thus, postoperative evaluation of the coronary arteries is also important.

Several studies have reported the clinical benefit of CTA for assessment of the coronary arteries in children with CHD [3-6]. However, most of them focused on prospective electrocardiography (ECG)-gated cardiac imaging. Although the ECG-gating technique, which provides proper ECG phase selection, is the standard technique for cardiac imaging, the use of ECG is more time consuming in patient preparation and artifacts can arise from ECG electrodes. Children with CHD frequently have extracardiac malformations and the assessment of these malformations is also important. Artifacts from ECG electrodes can be an obstacle when evaluating extracardiac structures.

In adults, high-pitch dual-source computed tomography (DSCT) makes the proximal segments of the coronary arteries accessible even without the application of ECG gating [7]. In children, on the other hand, although the usefulness of high-pitch DSCT without ECG gating has been reported in the assessment of CHD [8], there is a limited study focusing on coronary artery visibility in pediatric patients with non-ECG-gated high-pitch DSCT. In addition, factors affecting the image quality of the

coronary arteries in children with CHD have not been fully investigated. Accordingly, the purpose of this study was to evaluate the image quality of the coronary arteries on non-ECG-gated high-pitch DSCT in children with CHD and to assess factors affecting image quality.

Methods

Patients

The institutional review board approved this study and waived the requirement for informed consent because of the study's retrospective nature.

We retrospectively reviewed 174 consecutive children up to 6 years of age who underwent non-ECG-gated high-pitch DSCT between January 2014 and March 2015 for evaluation of known or suspected CHD or for postoperative follow-up. Thirty-two patients who did not undergo ECG within 1 month before the CT examination were excluded. Consequently, 142 patients (83 boys, 59 girls; mean age: 26.4 ± 23.4 months, range: 1 day to 83 months; mean body weight: 9.13 ± 4.74 kg, range: 2.0 to 31.2 kg) were included in this study.

CT protocol

All examinations were performed with a dual-source CT scanner (Somatom Definition Flash, Siemens Healthcare, Forchheim, Germany) without ECG gating. All patients were scanned during free breathing. Short-acting sedation was performed if necessary.

A non-ionic low-osmolar contrast medium (Iopamiron 300, Bayer, Osaka, Japan) was injected via the peripheral veins with a power injector at a volume of 2 mL/kg of body weight (600 mg iodine/kg). The injection rate was 0.5–1.5 mL/s depending on body weight. The scan was started 2

seconds after the contrast media injection. CT parameters were as follows: pitch, 3.2; gantry rotation time, 0.28 s; slice collimation, $2 \times 128 \times 0.6$ mm using a z-flying focal spot technique; automated tube voltage (Care kV, Siemens Healthcare); scout-based automatic reference tube current selection (CareDose 4D, Siemens Healthcare); and 75 milliseconds of temporal resolution. All images were reconstructed with an iterative reconstruction algorithm (sonogram-affirmed iterative reconstruction, SAFIRE; Siemens Healthcare). A normal soft tissue reconstruction kernel (I36) was used with a section thickness of 0.6 mm and a reconstruction interval of 0.3 mm.

Image processing analysis

All images were transferred to a processing workstation (Synapse Vincent; Fujifilm Medical Systems, Tokyo, Japan). Volume rendering (VR) and multiplanar reformation (MPR) were used for image interpretation. All images were evaluated by two radiologists independently who were blinded to patient history and ECG, coronary angiography, and surgical findings. The image qualities of four segments of the coronary arteries—the proximal right coronary artery (RCA), left main artery (LM), proximal left anterior descending artery (LAD), and proximal left circumflex artery (LCX)—were visually analyzed. The definition of “proximal” depends on length and location. Distal segments were not included in this evaluation because assessment of the distal coronary artery segments is not always necessary to identify CAA [3].

Image quality was evaluated using a five-point scale as follows [5]: 5, clear visualization without any motion artifacts; 4, mild motion artifacts but high diagnostic confidence; 3, obvious blurring, moderate diagnostic confidence; 2, identified but equivocal, may simulate other structures; and 1, severe blurring, no coronary artery segment can be visualized (no useful information obtained) (Fig. 1). In the case of

discordance between the two radiologists, the lower score was used. Scores of 3, 4, and 5 were considered sufficient diagnostic image quality.

Radiation dose estimates

The volume CT dose index (CTDI_{vol}) and dose-length product (DLP) were obtained systematically from CT. The CTDI_{vol} and DLP were obtained for a 32-cm phantom. To calculate the effective dose (mSv), the DLP was multiplied by a scanner-specific conversion factor provided by the manufacturer to adapt it to a 16-cm phantom: 2.4 for 70 kV, 2.3 for 80 kV, and 2.2 for 100 kV. This value was then multiplied by the age-specific conversion coefficient for the chest: 0.039 mSv/(mGy·cm) for children up to 4 months, 0.026 mSv/(mGy·cm) for those 4 months to 3 years of age, and 0.018 mSv/(mGy·cm) for those 3–6 years of age [9].

Statistical analysis

Image quality scores and continuous variables are expressed as the mean \pm standard deviation (SD) and categorical variables are expressed as percentages. Inter-observer agreement regarding image quality of the coronary artery segments was evaluated with weighted kappa statistics as follows: $\kappa = 0.41\text{--}0.60$, moderate agreement; $\kappa = 0.61\text{--}0.80$, substantial agreement; and $\kappa \geq 0.81$, almost perfect agreement [10].

Heart rate data were obtained from the ECG examination performed within 1 month before the CT examination. Age, body weight, and heart rate were evaluated between two groups—patients with good diagnostic image quality in all four segments and patients with at least one segment with non-diagnostic image quality—using the Mann-Whitney U test. Predictors of image quality were assessed by a multivariate logistic regression, including age, body weight, and heart rate between two groups—patients

with good diagnostic image quality in all four segments and patients with at least one segment with non-diagnostic image quality. Statistical analysis was performed with SPSS version 22.0 (SPSS, Chicago, IL, USA) and R version 3.1.2 (The R Foundation for Statistical Computing, Vienna, Austria). Values of $p < 0.05$ were considered statistically significant. A variance inflation factor (VIF) was used to assess multicollinearity. A VIF value exceeding 10 was regarded as indicating severe multicollinearity.

Results

Patient demographics and radiation dose parameters are presented in Table 1. The mean heart rate was 117 ± 23 beats/min (range: 36–125 beats/min). The mean CTDI_{vol} was 0.83 ± 0.35 mGy (range: 0.28–2.44 mGy), the mean DLP was 22.5 ± 11.8 mGy·cm (range: 6–78 mGy·cm), and the mean effective dose was 1.30 ± 0.57 mSv (range: 0.56–3.53 mSv). The diagnoses of the patients are described in Table 2. Coronary anomalies were found in 13 patients: seven patients had the left coronary artery from the right sinus of Valsalva, one had the RCA from the left sinus of Valsalva, two had the LCX from the RCA, one had the LAD from the RCA, one had the RCA from the LCX, and one had angiectopia of the LCX.

A total of 568 coronary artery segments were evaluated. The mean image quality scores were 3.48 ± 1.25 for observer 1 and 3.44 ± 1.04 for observer 2. The level of agreement between the two observers was substantial ($\kappa = 0.71$). All cases with discordant scores had only a one-point difference. Image quality scores and diagnostic rates for the coronary artery segments are shown in Table 3. Of all 568 segments, 457 (80.5%) were considered to have diagnostic image quality. Non-diagnostic image quality was most frequently observed in the proximal LCX (40.8%) and less frequently in the LM (7.0%). In 76 patients (53.5%), all four segments were observed to have diagnostic image quality. Sixty-six patients (46.5%) had at least one non-diagnostic coronary segment, 35 patients had one non-diagnostic

segment, 20 patients had two non-diagnostic segments, eight patients had three non-diagnostic segments, and in three patients, all four segments were non-diagnostic.

Patients with non-diagnostic segments were significantly younger (21.6 ± 25.5 months), had a lower body weight (7.82 ± 5.00 kg), and had a faster heart rate (123 ± 23.7 beats/min) (each $p < 0.05$) than patients with diagnostic image quality of all four segments (30.6 ± 20.7 months, 10.3 ± 4.20 kg, and 113 ± 21.6 beats/min, respectively) (Table 4).

The results of the multivariate logistic regression to predict image quality of the coronary artery segments are listed in Table 5. Multicollinearity was absent because the VIF values for all independent factors were less than 6. Body weight was a significant predictor of coronary artery segment image quality (odds ratio, 1.228; $p = 0.029$).

Discussion

Our study showed that 80.5% of the proximal segments of the coronary arteries had diagnostic image quality on non-ECG-gated high-pitch DSCT, which implies that this modality is feasible for evaluating the coronary arteries in children with CHD. The percentage of patients with diagnostic image quality in all four segments was 53.5%. In cases such as complete TGA, in which detailed evaluation of the anatomy of the coronary arteries is necessary, this might be insufficient as preoperative information. The LM was the most well-visualized segment. The proximal LCX had the lowest image quality scores, which seemed to be caused by its small size.

There have been two reports on the image quality of non-ECG-gated DSCT of the coronary arteries in children. Ben Saad et al. [11] reported that the diagnostic rates of the left and right coronary arteries on non-ECG-gated DSCT with a pitch of 1.4 were 43% and 15%, respectively. Bridoux et al. [12]

reported that 36.5% of proximal coronary artery segments were detected with non-ECG-gated DSCT with a pitch of 2.0. The older ages of the patients in our study could be one of the reasons why the proximal artery segments were better identified than those identified in prior studies. In addition, using a higher pitch of 3.2, which contributes to high temporal resolution, might have led to better image quality of the coronary arteries in our study. On the other hand, several studies have reported coronary artery image quality on ECG-gated DSCT in children with CHD. Ben Saad et al. [11] reported that 91% of proximal left coronary artery and 84% of RCA images had diagnostic image quality. Goo et al. [13] reported that 97.1% of the origin and proximal segments of the coronary arteries were identified. Pache et al. [14] found that 77.3% of the coronary arteries were detectable in their proximal and middle courses. The study by Nie et al. [5] showed that 70% of the proximal and middle segments of the coronary arteries had sufficient image quality. Although our study should not be simply compared with these studies because the patient demographics and the assessment tools were different, it seems that ECG-gated DSCT provided higher image quality of the proximal coronary arteries than that obtained with non-ECG-gated high-pitch DSCT. However, non-ECG-gated high-pitch DSCT has an advantage in the assessment of extracardiac structures because of the lack of artifacts from electrodes. Given that 80.5% of the proximal segments of the coronary arteries had diagnostic image quality even on non-ECG-gated high-pitch DSCT, non-ECG-gated high-pitch DSCT might be an alternative to ECG-gated DSCT, particularly when assessment of the extracardiac structures is as essential as assessment of the coronary arteries.

In our study, a multivariate logistic regression indicated that body weight was an independent factor affecting the image quality of the coronary arteries. It is assumed that the image quality of the coronary arteries was deteriorated in patients with lower body weights because they had smaller body sizes and therefore spatial resolution was decreased. Previous studies [3,15,16] have reported that age was

also a factor affecting the image quality of the coronary arteries, but it is suspected that age also reflects body size, and likewise, body weight. Although Stoltzman et al. [17] reported that in adults, heart rate was a factor affecting the image quality of the coronary arteries, even on high-pitch DSCT, heart rate was not an independent factor in children with CHD in the present study. In children up to 6 years of age with CHD such as in our study, spatial resolution may influence the image quality of the coronary arteries more strongly than temporal resolution.

We used a high-pitch mode, which lowers the radiation dose more greatly than a sequential mode [5]. In addition, we used lower kV values and iterative reconstruction, which improve image quality [18]. Thus, we achieved a low effective dose of 1.30 ± 0.59 mSv while maintaining image quality sufficient for diagnosis. Previous studies likewise showed a reduction in the radiation dose on DSCT. Pache et al. [14] reported that the mean effective dose for prospective ECG-gated DSCT in children with CHD (mean age, 1.2 ± 1.1 years and mean body weight, 8.0 ± 3.7 kg) was 0.32 ± 0.11 mSv. Ben Saad et al. [11] reported that the mean effective doses in children with CHD (mean age, 132 days and mean body weight, 5.2 kg) were 0.5 ± 0.2 mSv and 1.3 ± 0.6 mSv for non-ECG-gated DSCT and ECG-gated DSCT, respectively. Compared with these studies, patients included in our study were older and weighed more than patients included in the previous studies, which seemed to result in a higher effective dose.

Our study has several limitations. First, this was a retrospective study performed at a single institution. In addition, we did not compare the image quality of the coronary arteries with that obtained using ECG-gated DSCT because the number of patients that underwent ECG-gated DSCT was small and the backgrounds of the patients that underwent ECG-gated DSCT were different from those of the patients included in this study. Heart rate data were not obtained during the CT scans. We adopted a lower image quality score in cases of discordance between the two radiologists. A stricter assessment of

image quality may lead to a lower diagnostic rate of coronary artery segments. We did not assess the diagnostic accuracy of the coronary arteries on the non-ECG-gated high-pitch DSCT because invasive coronary angiography was not performed for most patients included in this study. Finally, we assessed the “proximal” segments of the coronary arteries and did not evaluate detailed coronary anatomy that surgeons would require before operating. Further studies are needed to assess the entire coronary artery anatomy.

In conclusion, non-ECG-gated high-pitch DSCT provided feasible image quality of the coronary arteries in children with CHD at a low radiation dose. Lower body weight reduced the image quality of the coronary arteries.

Conflict of Interest: The authors declare that they have no conflict of interest.

Ethical approval: All procedures performed in studies involving human participants were in accordance with the ethical standards of the institutional and/or national research committee and with the 1964 Helsinki declaration and its later amendments or comparable ethical standards. For this type of study, formal consent is not required.

References

1. Goo HW, Seo DM, Yun TJ, Park JJ, Park IS, Ko JK, Kim YH (2009) Coronary artery anomalies and clinically important anatomy in patients with congenital heart disease: multislice CT findings. *Pediatr Radiol* 39:265-273. doi: 10.1007/s00247-008-1111-7
2. Angeli E, Formigari R, Pace Napoleone C, Oppido G, Ragni L, Picchio FM, Gargiulo G (2010) Long-term coronary artery outcome after arterial switch operation for transposition of the great arteries. *Eur J Cardiothorac Surg* 38:714-720. doi: 10.1016/j.ejcts.2010.03.055
3. Goo HW, Park IS, Ko JK, Kim YH, Seo DM, Yun TJ, Park JJ (2005) Visibility of the origin and proximal course of coronary arteries on non-ECG-gated heart CT in patients with congenital heart disease. *Pediatr Radiol* 35:792-798. doi: 10.1007/s00247-005-1482-y
4. Tsai IC, Lee T, Chen MC, Fu YC, Jan SL, Wang CC, Chang Y (2007) Visualization of neonatal coronary arteries on multidetector row CT: ECG-gated versus non-ECG-gated technique. *Pediatr Radiol* 37:818-825. doi: 10.1007/s00247-007-0512-3
5. Nie P, Wang X, Cheng Z, Ji X, Duan Y, Chen J (2012) Accuracy, image quality and radiation dose comparison of high-pitch spiral and sequential acquisition on 128-slice dual-source CT angiography in children with congenital heart disease. *Eur Radiol* 22:2057-2066. doi: 10.1007/s00330-012-2479-1
6. Jadhav SP, Golriz F, Atweh LA, Zhang W, Krishnamurthy R (2015) CT angiography of neonates and infants: comparison of radiation dose and image quality of target mode prospectively ECG-gated 320-MDCT and ungated helical 64-MDCT. *AJR Am J Roentgenol* 204:W184-W191. doi: 10.2214/AJR.14.12846

7. de Malherbe M, Duhamel A, Tacelli N, Hachulla AL, Pontana F, Faivre JB, Remy J, Remy-Jardin M (2012) Ultrafast imaging of the entire chest without ECG synchronisation or beta-blockade: to what extent can we analyse the coronary arteries? *Insights Imaging* 3:73-79. doi: 10.1007/s13244-011-0133-0
8. Han BK, Lindberg J, Grant K, Schwartz RS, Lesser JR (2011) Accuracy and safety of high pitch computed tomography imaging in young children with complex congenital heart disease. *Am J Cardiol* 107:1541-1546. doi: 10.1016/j.amjcard.2011.01.065
9. Thomas KE, Wang B (2008) Age-specific effective doses for pediatric MSCT examinations at a large children's hospital using DLP conversion coefficients: a simple estimation method. *Pediatr Radiol* 38:645-656. doi: 10.1007/s00247-008-0794-0
10. Landis JR, Koch GG (1977) The measurement of observer agreement for categorical data. *Biometrics* 33:159-174.
11. Ben Saad M, Rohnean A, Sigal-Cinqualbre A, Adler G, Paul JF (2009) Evaluation of image quality and radiation dose of thoracic and coronary dual-source CT in 110 infants with congenital heart disease. *Pediatr Radiol* 39:668-676. doi: 10.1007/s00247-009-1209-6
12. Bridoux A, Hutt A, Faivre JB, Flohr T, Duhamel A, Pagniez J, Remy J, Remy-Jardin M (2015) Coronary artery visibility in free-breathing young children on non-gated chest CT: impact of temporal resolution. *Pediatr Radiol* 45:1761-1770. doi: 10.1007/s00247-015-3401-1
13. Goo HW, Yang DH (2010) Coronary artery visibility in free-breathing young children with congenital heart disease on cardiac 64-slice CT: dual-source ECG-triggered sequential scan vs. single-source non-ECG-synchronized spiral scan. *Pediatr Radiol* 40:1670-1680. doi: 10.1007/s00247-010-1693-8

14. Pache G, Grohmann J, Bulla S, Arnold R, Stiller B, Schlensak C, Langer M, Blanke P (2011)

Prospective electrocardiography-triggered CT angiography of the great thoracic vessels in infants and toddlers with congenital heart disease: feasibility and image quality. *Eur J Radiol* 80:e440-e445. doi: 10.1016/j.ejrad.2011.01.032
15. Yu FF, Lu B, Gao Y, Hou ZH, Schoepf UJ, Spearman JV, Cao HL, Sun ML, Jiang SL (2013)

Congenital anomalies of coronary arteries in complex congenital heart disease: diagnosis and analysis with dual-source CT. *J Cardiovasc Comput Tomogr* 7:383-390. doi: 10.1016/j.jcct.2013.11.004
16. Tada A, Sato S, Kanie Y, Tanaka T, Inai R, Akagi N, Morimitsu Y, Kanazawa S (2016) Image quality of coronary computed tomography angiography with 320-row area detector computed tomography in children with congenital heart disease. *Pediatr Cardiol* 37:497-503. doi: 10.1007/s00246-015-1305-3
17. Stolzmann P, Goetti RP, Maurovich-Horvat P, Hoffmann U, Flohr TG, Leschka S, Alkadhi H (2011) Predictors of image quality in high-pitch coronary CT angiography. *AJR Am J Roentgenol* 197:851-858. doi: 10.2214/AJR.10.6072
18. Nakagawa M, Ozawa Y, Sakurai K, Shimohira M, Ohashi K, Asano M, Yamaguchi S, Shibamoto Y (2015) Image quality at low tube voltage (70 kV) and sinogram-affirmed iterative reconstruction for computed tomography in infants with congenital heart disease. *Pediatr Radiol* 45:1472-1479. doi: 10.1007/s00247-015-3372-2

Figure legends

Fig. 1 Cardiac computed tomography (CT) images demonstrate the five-point scale used for the assessment of image quality of the coronary arteries

a Score 5: A 31-month-old girl after total repair of pulmonary atresia with a ventricular septal defect and major aortopulmonary collaterals. The left main artery (LM) is clearly visualized without any motion artifacts (*arrow*). (Ao, aorta; PA, pulmonary artery; RPA, right pulmonary artery; RPV, right pulmonary vein; LPV, left pulmonary vein; SVC, superior vena cava; DA, descending aorta)

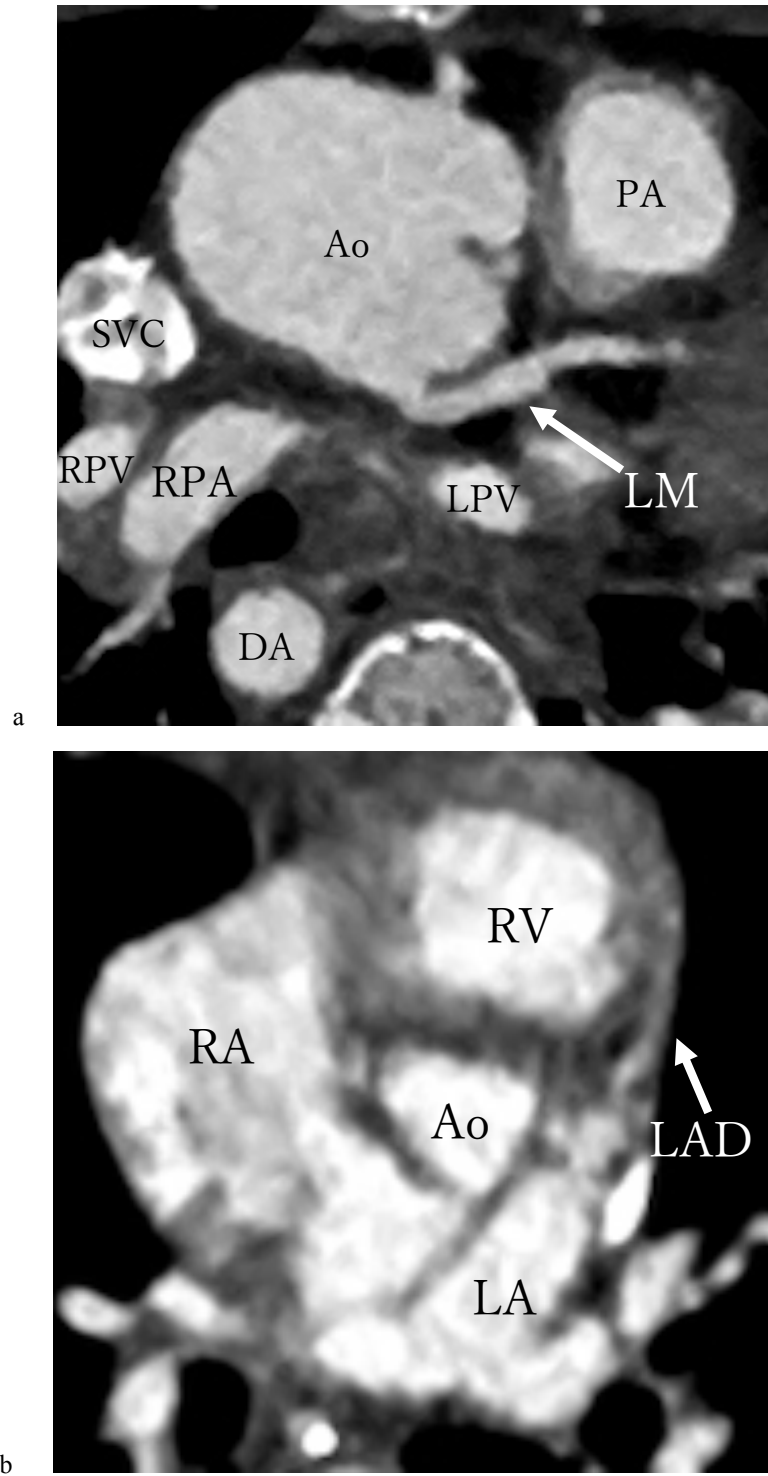
b Score 4: A 6-day-old girl with a diagnosis of hypoplastic left heart syndrome. The proximal left anterior descending artery (LAD) has mild motion artifacts but high diagnostic confidence (*arrow*). (Ao, aorta; RA, right atrium; LA, left atrium; RV, right ventricle)

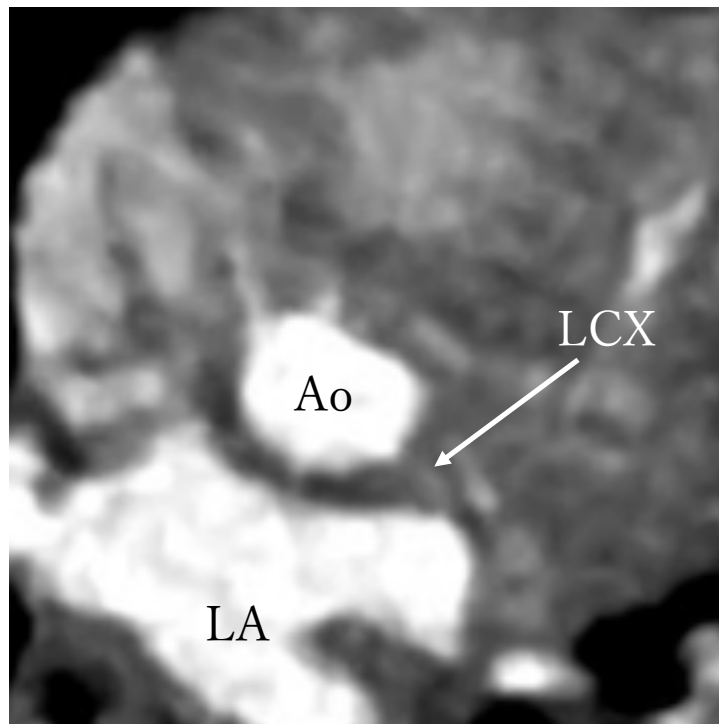
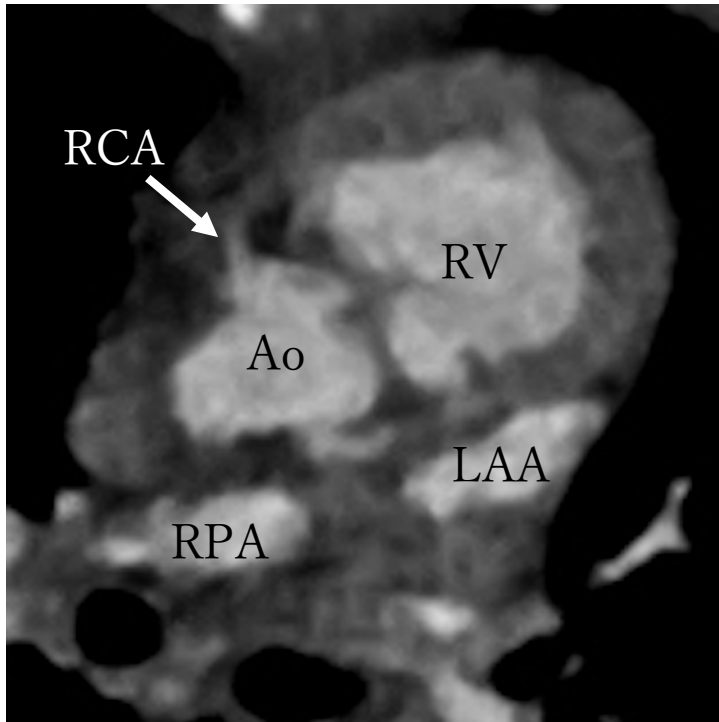
c Score 3: A 45-day-old boy after repair of a total anomalous pulmonary venous connection. The proximal right coronary artery (RCA) has mild motion artifacts but high diagnostic confidence (*arrow*). (Ao, aorta; RV, right ventricle; RPA, right pulmonary artery; LAA, left atrial appendage)

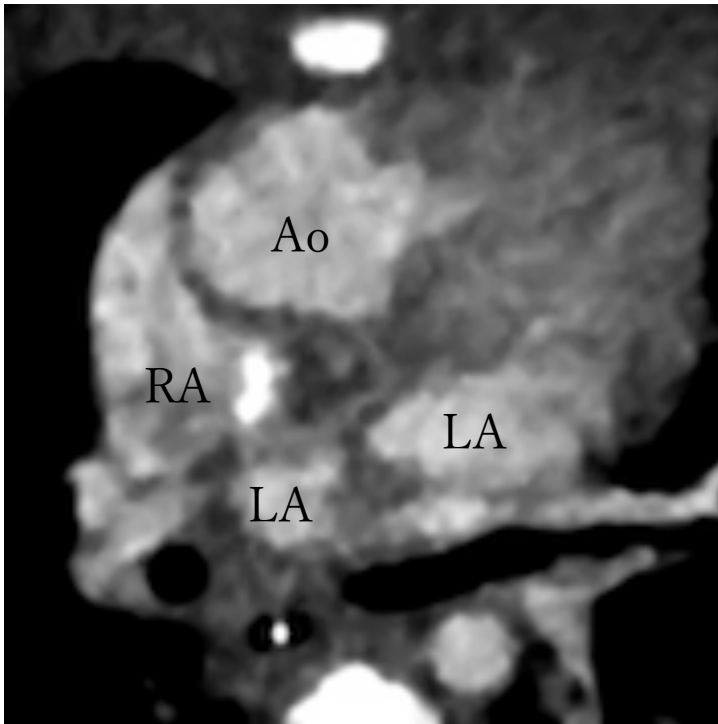
d Score 2: A 32-day-old boy with a diagnosis of coarctation of the aorta. The proximal left circumflex artery (LCX) can be recognized but is equivocal (*arrow*). It may simulate other structures. (Ao, aorta; LA, left atrium)

e Score 1: A 32-day-old boy with a diagnosis of congenitally corrected transposition of the great arteries. No proximal segment can be recognized. (Ao, aorta; RA, right atrium; LA, left atrium)

Fig. 1







e

Table 1 Patient demographics and radiation dose parameters

| Variable | Value |
|---------------------------|--------------------|
| Mean age | 26.4 ± 23.4 months |
| Mean body weight | 9.13 ± 4.74 kg |
| Mean heart rate | 117 ± 23 beats/min |
| Mean volume CT dose index | 0.83 ± 0.35 mGy |
| Mean dose-length product | 22.5 ± 11.8 mGy·cm |
| Mean effective dose | 1.30 ± 0.57 mSv |

Results are reported as the mean ± standard deviation unless otherwise specified.

CT: computed tomography

Table 2 Diagnoses of the patients

| Diagnosis | No. |
|---|-----|
| Hypoplastic left heart syndrome | 25 |
| Double outlet right ventricle | 21 |
| Single ventricle | 15 |
| Coarctation of the aorta | 13 |
| Tetralogy of Fallot | 10 |
| Pulmonary atresia with a ventricular septal defect | 10 |
| Pulmonary atresia with an intact ventricular septum | 6 |
| Corrected transposition of the great arteries | 4 |
| Ventricular septal defect | 4 |
| Persistent truncus arteriosus | 4 |
| Total anomalous pulmonary venous connection | 4 |
| Others | 26 |

No.: number of patients

Table 3 Image quality scores of the coronary artery segments

| Coronary artery segment | Image quality score | Diagnostic rate |
|--------------------------------|---------------------|-----------------|
| Overall | 3.30 ± 1.13 | 80.5% (457/568) |
| Proximal right coronary artery | 3.30 ± 1.13 | 81.0% (115/142) |
| Left coronary artery | | |
| Left main | 3.85 ± 0.96 | 93.0% (132/142) |
| proximal LAD | 3.37 ± 0.93 | 88.7% (126/142) |
| proximal LCX | 2.68 ± 1.16 | 59.2% (84/142) |

LAD: left anterior descending artery

LCX: left circumflex artery

Results are reported as the mean ± standard deviation unless otherwise specified.

Table 4 Univariate analysis of baseline variables and image quality of the coronary segments

Age, body weight, and heart rate were evaluated between two groups—patients with good diagnostic image quality in all four segments and patients with at least one segment with non-diagnostic image quality—using the Mann-Whitney U test.

| Variables | Patients with diagnostic | Patients with non-diagnostic | <i>p</i> |
|------------------|--------------------------|------------------------------|----------|
| | segments (n =76) | segments (n = 66) | |
| Age (months) | 30.6 ± 20.7 | 21.6 ± 25.5 | 0.001 |
| Body weight (kg) | 10.3 ± 4.20 | 7.82 ± 5.00 | 0.001 |
| Heart rate | | | |
| (beats/min) | 113 ± 21.6 | 123 ± 23.7 | 0.002 |

Results are reported as the mean ± standard deviation unless otherwise specified.

Table 5 Multivariate analysis for the prediction of image quality of the coronary segments

Predictors of image quality were assessed by a multivariate logistic regression between two groups—patients with good diagnostic image quality in all four segments and patients with at least one segment with non-diagnostic image quality.

| Parameter | β -Coefficient | Odds ratio | 95% CI | <i>p</i> |
|------------------------|----------------------|------------|-------------|----------|
| Age (months) | -0.28 | 0.973 | 0.936–1.009 | 0.136 |
| Body weight (kg) | 0.206 | 1.228 | 1.021–1.477 | 0.029 |
| Heart rate (beats/min) | -0.015 | 0.985 | 0.966–1.005 | 0.142 |

CI: confidence interval